Forschungszentrum Karlsruhe
Technik und Umwelt

Wissenschaftliche Berichte
FZKA 5838

Stress Intensity Factors, T-stress and Weight Functions for Double-edge-cracked Plates

T. Fett
Institut für Materialforschung

November 1996

FORSCHUNGSZENTRUM KARLSRUHE
Technik und Umwelt
Wissenschaftliche Berichte
FZKA 5838

Stress intensity factors, T-stress and weight functions for double-edge-cracked plates

T. Fett

Institut für Materialforschung

Forschungszentrum Karlsruhe GmbH, Karlsruhe
1996

Forschungszentrum Karlsruhe GmbH
Postfach 3640, 76021 Karlsruhe

ISSN 0947-8620

Abstract

This report deals with the determination of stress intensity factors, T-stress, and weight function for the double-edge-cracked plate by application of the Boundary Collocation procedure.
In the first part the fracture mechanical parameters are computed for several relative crack depths and different ratios of plate length to plate width and compiled in the form of tables. The second part deals with the first derivative of the weight function at the crack mouth which is used in the literature for application of the Petroski-Achenbach procedure.

Spannungsintensitätsfaktoren, T-Spannung und Gewichtsfunktion für die Platte mit beidseitigem Außenriß

Zusammenfassung

Es werden die Spannungsintensitätsfaktoren, Gewichtsfunktionen und der T-Spannungsterm für rechteckige Platten mit beidseitigem Außenriß mittels der "Boundary Collocation"-Prozedur ermittelt.
Im ersten Teil wird der Einfluß der relativen Rißlänge und des Verhältnisses von Probenhöhe zu Probenbreite untersucht. Der zweite Teil befaßt sich mit der ersten Ableitung der Gewichtsfunktion, die in der neueren Literatur zur Anwendung der approximativen Methode nach Petroski und Achenbach herangezogen wird.

Contents

1. Introduction

The fracture behaviour of cracked structures is dominated by the near-tip stress field. Sufficient information about the stresses is available if the stress intensity factor and the constant stress term, the T-stress, are known.
Stress intensity factors and T-stress are reported in handbooks for simple loading cases only, for instance pure tension and bending. In case of arbitrary stresses the weight function proposed by Bueckner [1] enables the related stress intensity factors to be computed. In a similar way, one can define a weight function (or Green's function) for T-stresses [2]-[4].
Handbook solutions for stress intensity factors and weight functions are restricted to ideal specimens, e.g. infinitely long plates. The aim of this report is to provide stress intensity factors, T-stress solutions, and weight functions for plates of various height/width ratios. In an earlier report the single-edge-cracked plate was investigated with respect to the stress intensity factor and T-stress [5]. In this report the double-edge-cracked plate is considered using the Boundary Collocation Method (BCM).
The condition of disappearing first derivative of the weight function at the crack mouth, being a point of special interest, is discussed in detail. The infinitely long double-edge-cracked plate is treated analytically and the finite plate is treated numerically.

2. General relations

2.1 Airy stress function, stresses and displacements

The total stress state in a cracked body is known if the Airy stress function Φ is available. The stress function can be obtained by solving the equation of compatibility

$$\Delta\Delta\Phi = 0 \tag{1}$$

For a cracked body a series representation for Φ was given by Williams [6]. Its symmetric part can be written

$$\begin{aligned}\Phi = \sigma^* W^2 \sum_{n=0}^{\infty} (r/W)^{n+3/2} A_n \left[\cos(n+3/2)\varphi - \frac{n+3/2}{n-1/2} \cos(n-1/2)\varphi \right] \\ + \sigma^* W^2 \sum_{n=0}^{\infty} (r/W)^{n+2} A_n^* [\cos(n+2)\varphi - \cos n\varphi]\end{aligned} \tag{2}$$

with the characteristic stress σ^* which may be the remote tensile stress in tensile tests or the outer fibre tensile stress in bending. The geometrical data are explained in fig.1. From the stress function the stress components can be computed by

$$\begin{aligned}\sigma_r &= \frac{1}{r}\frac{\partial\Phi}{\partial r} + \frac{1}{r^2}\frac{\partial^2\Phi}{\partial\varphi^2} \\ \sigma_\varphi &= \frac{\partial^2\Phi}{\partial r^2} \\ \tau_{r\varphi} &= \frac{1}{r^2}\frac{\partial\Phi}{\partial\varphi} - \frac{1}{r}\frac{\partial^2\Phi}{\partial r\partial\varphi}\end{aligned} \tag{3}$$

where r and φ are polar coordinates with the pole in the crack tip. One obtains

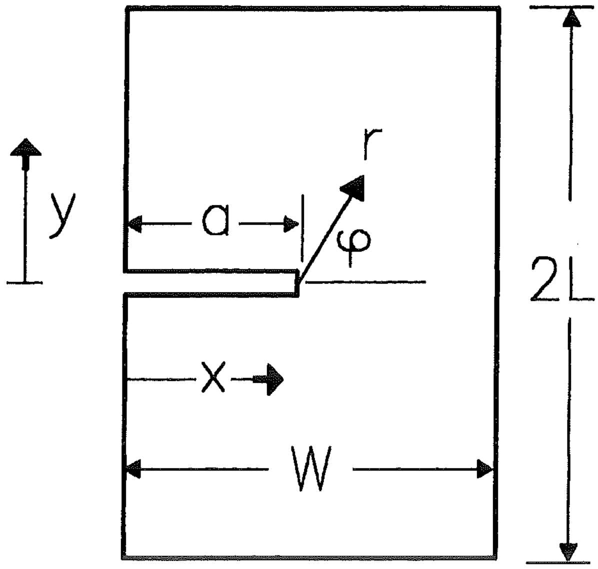

Figure 1. . Crack in a component; definition of polar coordinates.

$$\frac{\sigma_r}{\sigma^*} = \sum_{n=0}^{\infty} A_n \left(\frac{r}{W}\right)^{n-1/2} (n+3/2) \left[\frac{n^2 - 2n - 5/4}{n-1/2} \cos(n-1/2)\varphi - (n+1/2)\cos(n+3/2)\varphi \right]$$
$$+ \sum_{n=0}^{\infty} A_n^* \left(\frac{r}{W}\right)^{n} \left[(n^2 - n - 2)\cos n\varphi - (n+2)(n+1)\cos(n+2)\varphi \right] \tag{4}$$

$$\frac{\sigma_\varphi}{\sigma^*} = \sum_{n=0}^{\infty} A_n \left(\frac{r}{W}\right)^{n-1/2} (n+3/2)(n+1/2) \left[\cos(n+3/2)\varphi - \frac{n+3/2}{n-1/2} \cos(n-1/2)\varphi \right]$$
$$+ \sum_{n=0}^{\infty} A_n^* \left(\frac{r}{W}\right)^{n} (n+2)(n+1) \left[\cos(n+2)\varphi - \cos n\varphi \right] \tag{5}$$

$$\frac{\tau_{r\varphi}}{\sigma^*} = \sum_{n=0}^{\infty} A_n \left(\frac{r}{W}\right)^{n-1/2} (n+3/2)(n+1/2) \left[\sin(n+3/2)\varphi - \sin(n-1/2)\varphi \right]$$
$$+ \sum_{n=0}^{\infty} A_n^* \left(\frac{r}{W}\right)^{n} (n+1) \left[(n+2)\sin(n+2)\varphi - n \sin n\varphi \right] \tag{6}$$

The displacements u and v (u = radial component and v = angular component) can be calculated from the radial strains ε_r and tangential strains ε_φ. The following relations hold:

$$\varepsilon_r = \frac{\partial u}{\partial r} \tag{7}$$

$$\varepsilon_\varphi = \frac{u}{r} + \frac{1}{r}\frac{\partial v}{\partial \varphi} \tag{8}$$

From the Hooke's law in plane strain

$$\varepsilon_r = \frac{1}{E'}\sigma_r - \frac{\nu}{E'(1-\nu)}\sigma_\varphi \tag{9}$$

$$\varepsilon_\varphi = \frac{1}{E'}\sigma_\varphi - \frac{\nu}{E'(1-\nu)}\sigma_r \tag{10}$$

($E' = E/(1-\nu^2)$) and the stress components given by eq.(3) we obtain the following system of equations describing the displacements

$$E'\frac{\partial u}{\partial r} = \frac{1}{r}\frac{\partial \Phi}{\partial r} + \frac{1}{r^2}\frac{\partial^2 \Phi}{\partial \varphi^2} - \frac{\nu}{1-\nu}\frac{\partial^2 \Phi}{\partial r^2} \tag{11}$$

$$E'\left(\frac{u}{r} + \frac{1}{r}\frac{\partial v}{\partial \varphi}\right) = \frac{\partial^2 \Phi}{\partial r^2} - \frac{\nu}{1-\nu}\left(\frac{1}{r}\frac{\partial \Phi}{\partial r} + \frac{1}{r^2}\frac{\partial^2 \Phi}{\partial \varphi^2}\right) \tag{12}$$

After introducing the stress function, the integration of this system of differential equations leads to

$$\begin{aligned}\frac{u}{\sigma^* W} = {} & \frac{1+\nu}{E}\sum_{n=0}^{\infty} A_n (r/W)^{n+1/2}\frac{n+3/2}{n-1/2}\,\bullet \\ & \bullet\left[(n+4\nu-5/2)\cos(n-1/2)\varphi - (n-1/2)\cos(n+3/2)\varphi\right] \\ & + \frac{1+\nu}{E}\sum_{n=0}^{\infty} A_n^* (r/W)^{n+1}\left[(n+4\nu-2)\cos n\varphi - (n+2)\cos(n+2)\varphi\right]\end{aligned} \tag{13}$$

$$\begin{aligned}\frac{v}{\sigma^* W} = {} & \frac{1+\nu}{E}\sum_{n=0}^{\infty} A_n (r/W)^{n+1/2}\frac{n+3/2}{n-1/2}\,\bullet \\ & \bullet\left[(n-1/2)\sin(n+3/2)\varphi - (n-4\nu+7/2)\sin(n-1/2)\varphi\right] \\ & + \frac{1+\nu}{E}\sum_{n=0}^{\infty} A_n^* (r/W)^{n+1}\left[(n+2)\sin(n+2)\varphi - (n-4\nu+4)\sin n\varphi\right]\end{aligned} \tag{14}$$

The Cartesian components of the displacements are

$$u_x = u \cos\varphi - v \sin\varphi$$
$$u_y = u \sin\varphi + v \cos\varphi \tag{15}$$

The crack opening displacement field results for $\varphi = \pi$

$$v_{\varphi=\pi} = \frac{4}{E'} \sum_{n=0}^{\infty} A_n (a-x)^{n+1/2} \frac{n+3/2}{n-1/2} (-1)^{n+1} \tag{16}$$

The unknown coefficients A_n and A^* have to be determined for the special specimen/crack geometry and the chosen loading mode.

2.2 Stress intensity factor and T-stress

Especially for the stress component σ_x ahead of the crack ($\varphi = 0$), eq.(4) reads

$$\sigma_x / \sigma^* = -\sum_{n=0}^{\infty} 2A_n (r/W)^{n-1/2} \left(n + \frac{3}{2}\right) \frac{2n+1}{2n-1} - \sum_{n=0}^{\infty} 4A_n^* (r/W)^n (n-1) \tag{17}$$

In fracture mechanics most interest is focussed on the stress intensity factor characterising the singular stress field ahead of a crack tip. The related stress singularity is responsible mainly for the failure of cracked components. The stress intensity factor K_I is related to coefficient A_0 by

$$K_I = \sigma^* F \sqrt{\pi a} \quad , \quad F = \sqrt{18/\alpha}\, A_0 \ , \quad \alpha = a/W \tag{18}$$

with the geometric function F. As Larsson and Carlsson [7] showed very early, there is experimental evidence that also the constant stress contributions acting over a longer distance from the crack tip may affect fracture mechanics properties. The related coefficient A_0^* leads to the constant stress term. If no x-stress component is present in the uncracked structure, the total x-stress is given by the so-called T-stress T

$$\sigma_x = T = -4\sigma^* A_0^* \tag{19}$$

Following a suggestion by Leevers and Radon [8], the T-stress can be dimensionless expressed by the "stress biaxiality ratio" β

$$\beta = \frac{T\sqrt{\pi a}}{K_I} \tag{20}$$

or written in terms of coefficients A_0, A_0^* as

$$\beta = \frac{T}{\sigma^* F} = -\frac{4}{\sqrt{18}} \sqrt{\alpha}\, \frac{A_0^*}{A_0} \tag{21}$$

2.3 Computation of the weight function

The weight function method developed by Bueckner [1] simplifies the determination of stress intensity factors. If this function is known, the stress intensity factor can be obtained by simply multiplying this function by the stress distribution and integrating it along the crack length

$$K_I = \int_0^a \sigma(x) h(x,a)\, dx \tag{22}$$

The weight function $h(x,a)$ depends only on the geometry of the component. The relation of Rice [9]provides the weight function from the crack opening displacement $v(x,a)$ of any arbitrarily chosen loading and the corresponding stress intensity factor $K_I(a)$ according to

$$h(x,a) = \frac{E'}{K_I(a)} \frac{\partial}{\partial a} v(x,a) \tag{23}$$

The components of the weight function result as

$$h_x = \frac{E'}{K_r} \frac{\partial u_x}{\partial a} \qquad h_y = \frac{E'}{K_r} \frac{\partial u_y}{\partial a} \tag{24}$$

The derivatives in eq.(24) can be evaluated by

$$\begin{aligned}
\frac{du_x}{da} &= \frac{\partial u_x}{\partial r}\frac{dr}{da} + \frac{\partial u_x}{\partial \varphi}\frac{d\varphi}{da} + \frac{\partial u_x}{\partial A_n}\frac{dA_n}{da} + \frac{\partial u_x}{\partial A_n^*}\frac{dA_n^*}{da} \\
\frac{du_y}{da} &= \frac{\partial u_y}{\partial r}\frac{dr}{da} + \frac{\partial u_y}{\partial \varphi}\frac{d\varphi}{da} + \frac{\partial u_y}{\partial A_n}\frac{dA_n}{da} + \frac{\partial u_y}{\partial A_n^*}\frac{dA_n^*}{da}
\end{aligned} \tag{25}$$

with

$$\frac{dr}{da} = -\cos\varphi\,, \qquad \frac{d\varphi}{da} = \frac{\sin\varphi}{r} \tag{26}$$

2.4 Determination of the coefficients A_0 and A_0^*

A simple possibility of determination of the coefficients A_0 and A_0^* is the application of the Boundary Collocation Method (BCM). For practical application of eq.(2), which is used to determine A_0 and A_0^*, the infinite series must be truncated after the Nth term for which an adequate value must be chosen. The still unknown coefficients are determined by fitting the stresses and displacements to the specified boundary conditions. In case of the double-edge-cracked rectangular plate of half-width W and length $2L$ (fig.3) the conditions are

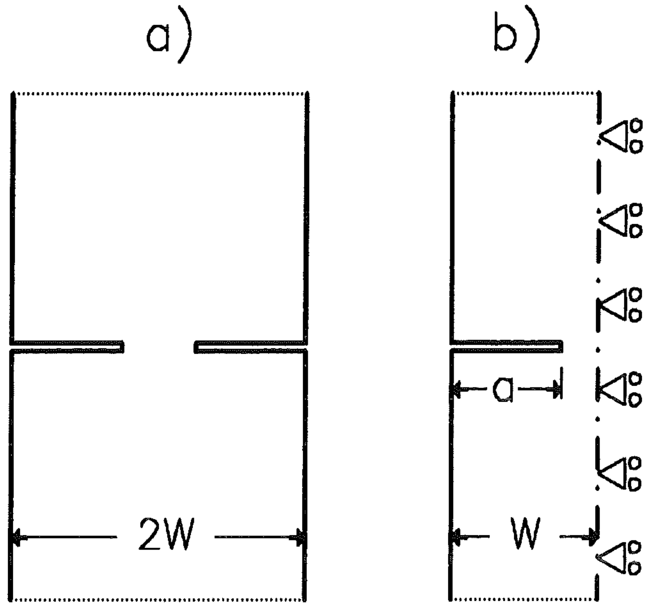

Figure 2. Geometry. a) Double-edge-cracked strip, b) half-specimen with symmetry boundary conditions.

$$\sigma_x = 0 \quad , \quad \tau_{xy} = 0 \quad \text{for} \quad x = 0 \tag{27}$$

$$\sigma_y = \sigma^* \quad , \quad \tau_{xy} = 0 \quad \text{for} \quad y = L \tag{28}$$

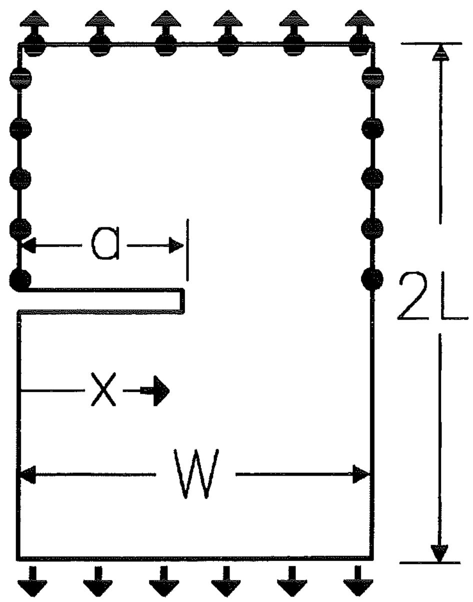

Figure 3. Boundary Collocation points. Left half of a double-edge-cracked plate with collocation points.

$$\frac{\partial u}{\partial x} = 0 \quad , \quad \tau_{xy} = 0 \quad \text{for} \quad x = W \tag{29}$$

About 100-120 coefficients for eq.(2) were determined from 800 stress equations given at 400 nodes along the outer contour (symbolised by the circles in fig.3). For a selected number of (N + 1) edge points the related stress components are computed, and we obtain a system of 2(N + 1) equations with 2(N + 1) unknowns whose solutions allow all 2(N + 1) coefficients of eq.(2) to be determined.

The expenditure in terms of computation can be reduced by selection of a rather large number of edge points and by solving subsequently the then overdetermined system of equations using the least squares of deviations so that a set of "best" coefficients is obtained. The Harwell subroutine V02AD is used here to determine the best fit.

3. Results

3.1 Crack opening displacements

Figure 4 shows the crack opening displacements for a plate of relative height $L/W = 1.7$ and several relative crack lengths. Near the free surface the curves are strongly parallel.

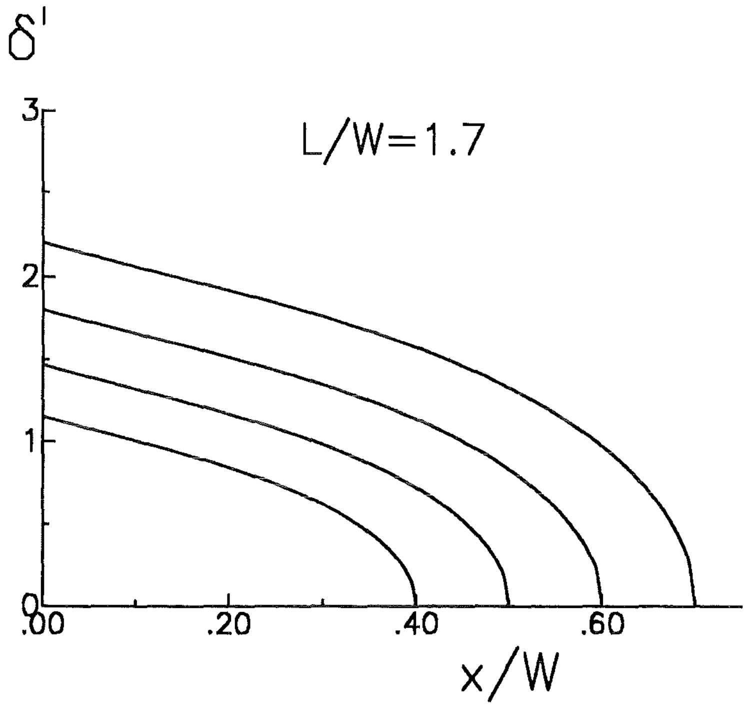

Figure 4. Crack opening displacements. Displacements under constant tractions σ_0 at the ends of the plate.

Figure 5 represents crack opening displacements for a constant crack length but different relative plate heights. From this diagram one can conclude that the shape of the crack opening displacement field depends significantly on the specimen height.

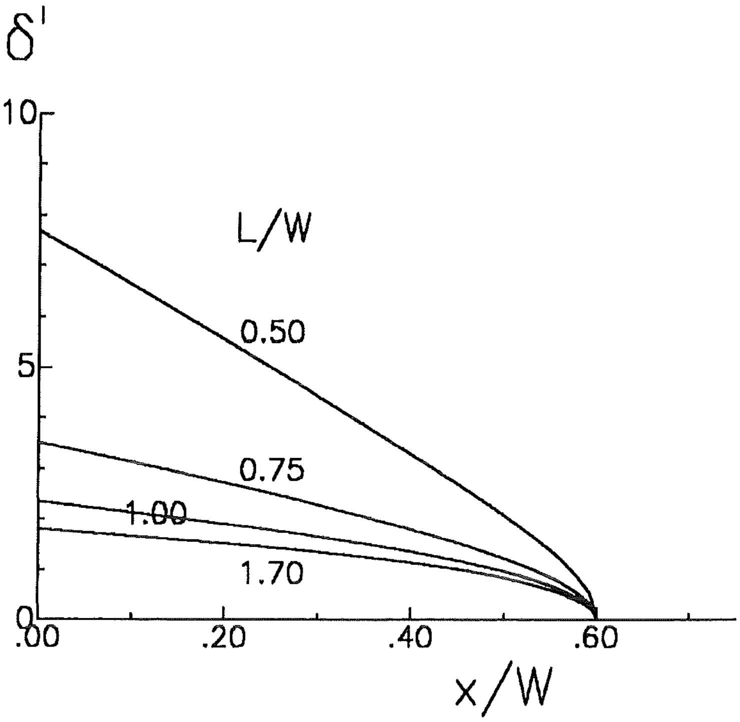

Figure 5. Crack opening displacements. Displacements under constant tractions σ_0 for $a/W=0.6$ and several relative plate lengths L/W. Normalisation: $\delta' = \delta E'/(\sigma_0 W)$.

3.2 Influence of plate length on stress intensity factor and T-stress

Double-edge-cracked rectangular plates were investigated under constant tensile stress. BCM-computations provided the coefficients A_0 and A_0^*. In Table 1 the geometric function F, computed from A_0 by eq.(18), is entered (see also fig.6). Table 2 gives the coefficient A_0^*. The biaxiality ratio is shown in Table 3.

α	$L/W=1.5$	1.25	1.00	0.75	0.50	0.25
0	1.1215	1.1215	1.1215	1.1215	1.1215	1.1215
0.3	0.94	0.96	1.029	1.180	1.496	2.468
0.4	0.8891	0.9171	0.9946	1.1926	1.646	2.970
0.5	0.8389	0.8659	0.9427	1.1537	1.7190	3.22
0.6	0.7900	0.8135	0.8760	1.0597	1.6529	3.25
0.7	0.7420	0.7492	0.8029	0.9297	1.4142	3.1544
1.0	0.6366	0.6366	0.6366	0.6366	0.6366	0.6366

Table 1. . Geometric function $F' = F\sqrt{1-\alpha}$.

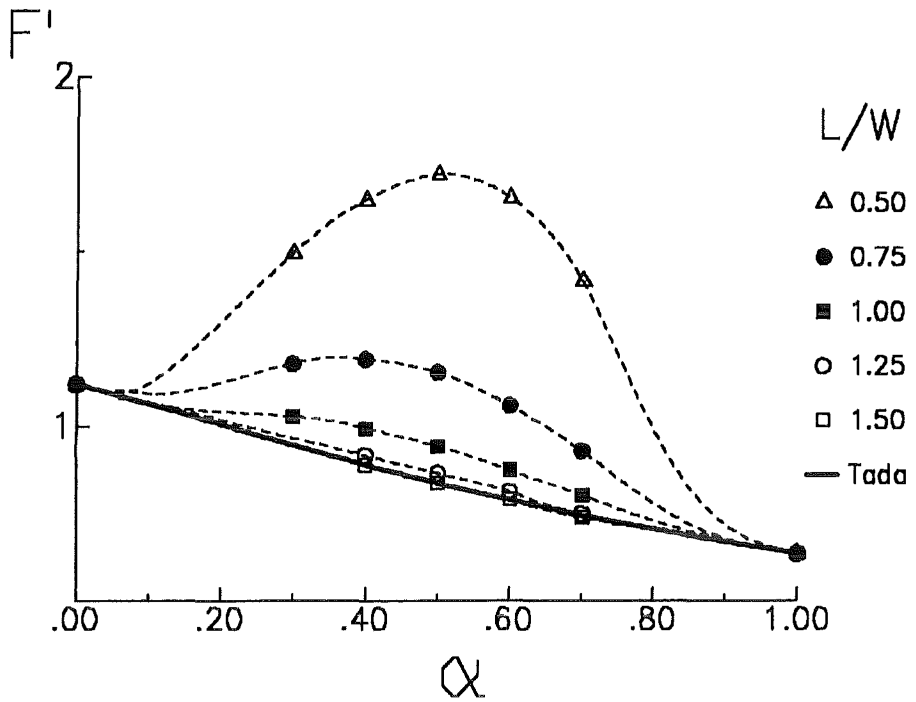

Figure 6. Stress intensity factor. Geometric function $F' = F\sqrt{1-\alpha}$.

α	$L/W = 1.5$	1.25	1.00	0.75	0.50	0.25
0	0.1315	0.1315	0.1315	0.1315	0.1315	0.1315
0.3	0.133	0.130	0.1279	0.1183	0.0642	-0.456
0.4	0.1321	0.1259	0.1101	0.0705	-0.064	-1.060
0.5	0.1304	0.1160	0.0791	-0.0112	-0.2645	-1.7817
0.6	0.1275	0.1023	0.0382	-0.1208	-0.5504	-2.425
0.7	0.1232	0.08	-0.0058	-0.2423	-0.9195	-3.2672

Table 2. . Coefficient A_0^*

α	$L/W = 1.5$	1.25	1.00	0.75	0.50	0.25
0	-0.469	-0.469	-0.469	-0.469	-0.469	-0.469
0.3	-0.472	-0.453	-0.416	-0.336	-0.144	0.618
0.4	-0.460	-0.425	-0.343	-0.183	0.120	1.106
0.5	-0.440	-0.379	-0.237	0.028	0.435	1.528
0.6	-0.408	-0.318	-0.110	0.288	0.842	1.862
0.7	-0.364	-0.228	0.016	0.571	1.424	2.269

Table 3. . Biaxiality ratio β, eq.(20).

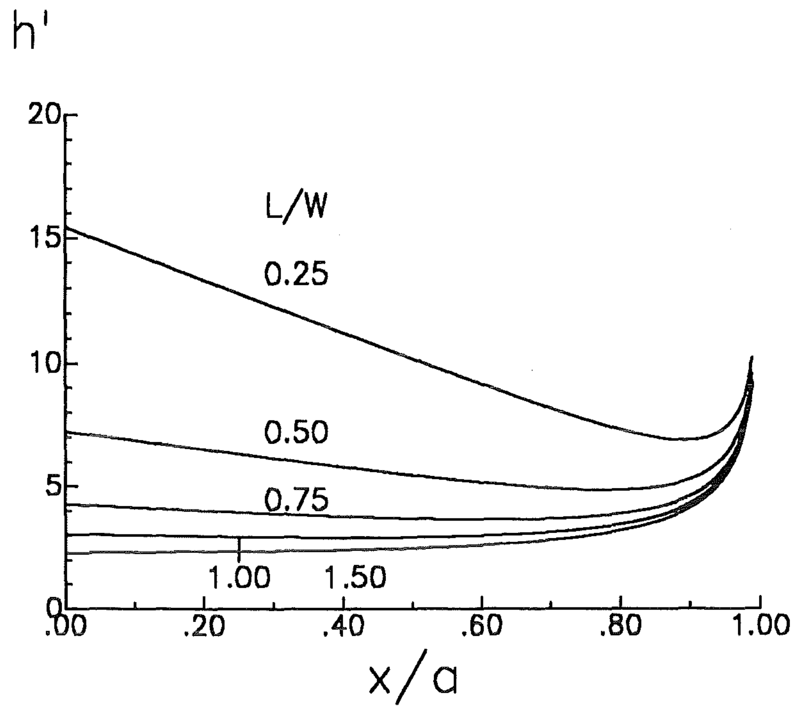

Figure 7. Weight function. Normalised representation $h' = h\sqrt{W}$

3.3 Weight function

From the crack opening displacements the weight function was computed using eq.(24). Figure 7 shows the weight function for several relative plate heights L/W. Single data in a normalised representation are entered in Tables 4-7.

x/a	$L/W=0.25$	0.50	0.75	1.00	1.50
0	15.4	7.21	4.27	3.04	2.35
0.1	13.6	6.49	3.92	2.84	2.24
0.2	11.9	5.80	3.58	2.64	2.13
0.3	10.2	5.12	3.24	2.44	2.01
0.4	8.67	4.47	2.91	2.24	1.90
0.5	7.17	3.84	2.60	2.06	1.79
0.6	5.76	3.25	2.29	1.88	1.68
0.7	4.45	2.69	2.01	1.71	1.57
0.8	3.25	2.16	1.73	1.54	1.47
0.9	2.16	1.68	1.49	1.40	1.37
1.0	1.262	1.262	1.262	1.262	1.262

Table 4. Weight function. Normalised representation $h\sqrt{W}\sqrt{1-x/a}$, **a/W=0.4**

x/a	$L/W=0.25$	0.50	0.75	1.00	1.50
0	16.8	7.84	4.20	2.89	2.30
0.1	14.8	7.01	3.85	2.70	2.18
0.2	12.9	6.20	3.49	2.51	2.06
0.3	11.1	5.43	3.14	2.31	1.93
0.4	9.4	4.68	2.80	2.12	1.81
0.5	7.73	3.97	2.48	1.93	1.69
0.6	6.15	3.30	2.17	1.75	1.56
0.7	4.68	2.68	1.87	1.58	1.45
0.8	3.33	2.10	1.60	1.41	1.33
0.9	2.13	1.56	1.35	1.26	1.22
1.0	1.128	1.128	1.128	1.128	1.128

Table 5. Weight function. Normalised representation $h\sqrt{W}\sqrt{1-x/a}$, **a/W=0.5**

x/a	$L/W=0.25$	0.50	0.75	1.00	1.50
0	19.4	7.91	4.00	2.79	2.17
0.1	17.1	7.04	3.66	2.61	2.06
0.2	14.8	6.21	3.31	2.42	1.95
0.3	12.6	5.40	2.98	2.23	1.84
0.4	10.6	4.63	2.65	2.04	1.72
0.5	8.66	3.90	2.33	1.86	1.60
0.6	6.83	3.21	2.03	1.68	1.49
0.7	5.11	2.57	1.75	1.51	1.25
0.8	3.55	1.99	1.48	1.34	1.25
0.9	2.16	1.45	1.24	1.18	1.14
1.0	1.030	1.030	1.030	1.030	1.030

Table 6. Weight function. Normalised representation $h\sqrt{W}\sqrt{1-x/a}$, **a/W=0.6**

x/a	$L/W=0.25$	0.50	0.75	1.00	1.50
0	25.6	7.47	3.69	2.77	1.95
0.1	22.3	6.65	3.39	2.59	1.86
0.2	19.1	5.85	3.09	2.41	1.77
0.3	16.1	5.09	2.78	2.23	1.68
0.4	13.3	4.35	2.49	2.05	1.58
0.5	10.7	3.65	2.20	1.86	1.48

0.6	8.22	[illegible]	1.93	1.68	1.38
0.7	5.98	2.39	1.66	1.50	1.27
0.8	3.99	1.84	1.41	1.32	1.17
0.9	2.29	1.36	1.18	1.13	1.06
1.0	0.954	0.954	0.954	0.954	0.954

Table 7. Weight function. Normalised representation $h\sqrt{W}\sqrt{1-x/a}$, **a/W=0.7**

3.4 The first derivative of the weight function

The numerical results of fig.7 suggest for $L/W>1$ that $\partial h/\partial x \simeq 0$ holds at the crack mouth. This condition has been used in the literature [10] for the application of the Petroski-Achenbach procedure [11]. One can prove this condition analytically.

3.4.1 The infinitely long strip

In order to compute the first derivative of the weight function for a double-edge-cracked plate (see fig.8) we consider this specimen under pairs of forces acting directly at the crack faces. The specimen is assumed to be cut out of an infinite array of collinear cracks in an infinite body (see fig.9) which are also loaded with concentrated forces at the crack faces. The cutting lines are the dash-dotted lines of fig.9. The total stress state in such a structure can be derived from the Westergaard stress function (see e.g. [12])

$$\Phi = \frac{2P}{W}\frac{\cos(\pi b/W)\sqrt{\sin^2(\pi a/W)-\sin^2(\pi b/W)}}{\left[\sin^2(\pi z/W)-\sin^2(\pi b/W)\right]\sqrt{1-\sin^2(\pi a/W)/\sin^2(\pi z/W)}} \tag{30}$$

with the geometric data a, b, and W as illustrated in fig.9. The complex variable z is given by $z = x + iy$ with the origin of x,y in the crack centre.
The σ_x-stresses are given by

$$\sigma_x(x,y,b) = \mathrm{Re}\,\Phi - y\,\mathrm{Im}\frac{d}{dz}\Phi \tag{31}$$

Therefore, the tractions which have to be applied at the surface $x=0$ of the double-edge-cracked plate to satisfy the displacement conditions occurring in the case of the internal crack are

$$\sigma_{appl} = -\sigma_x(0,y,b) \tag{32}$$

These surface tractions (illustrated schematically in fig.8 by the shaded areas) are responsible for the stress intensity factor ΔK_I which can be expressed by the weight function formulation [1]

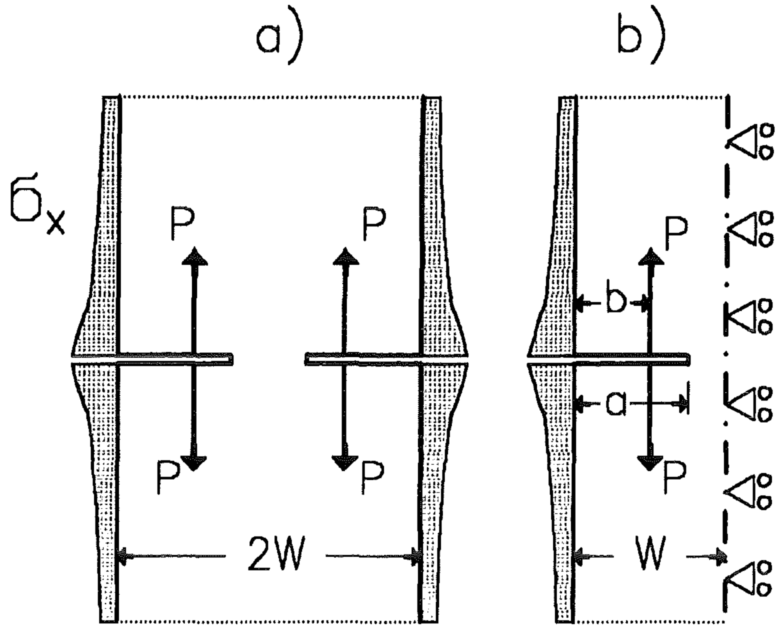

Figure 8. . a) Double-edge-cracked plate, b) symmetry conditions. Shaded areas: surface tractions which reproduce the stress state of the internal cracks for the same loads, see fig.9.

$$\Delta K_I = \int_0^\infty \sigma_x (0,y,b)\, h_{x,DE} (a,y)\, dy \tag{33}$$

where $h_{x,DE}$ is the weight function for tractions acting in x-direction. The subscript DE stands for "Double Edge" and subscript INT denotes the internal crack. On the other hand, the change in stress intensity factor caused by the free surface condition is given by

$$\Delta K_I = K_{I,DE} - K_{I,INT} = \int_0^a [h_{y,DE}(a,x) - h_{y,INT}(a,x)]\sigma_{y=0,x}\, dx \tag{34}$$

with the crack surface tractions σ_y acting normal to the crack. The crack-face weight functions are $h_{y,DE}$ for the double-edge crack and $h_{y,INT}$ for the internal crack.
The stress distribution of a pair of forces $\pm$P acting on the crack surface at $x = b$ is expressed in terms of the Dirac δ function as

$$\sigma_y (x) = P\, \delta(x - b) \tag{35}$$

(assuming the plate thickness $B = 1$). Introducing this in eq.(34) gives

$$\Delta K_I = P h_{y,DE} (a,b) \; - \; P h_{y,INT} (a,b) \tag{36}$$

and, finally,

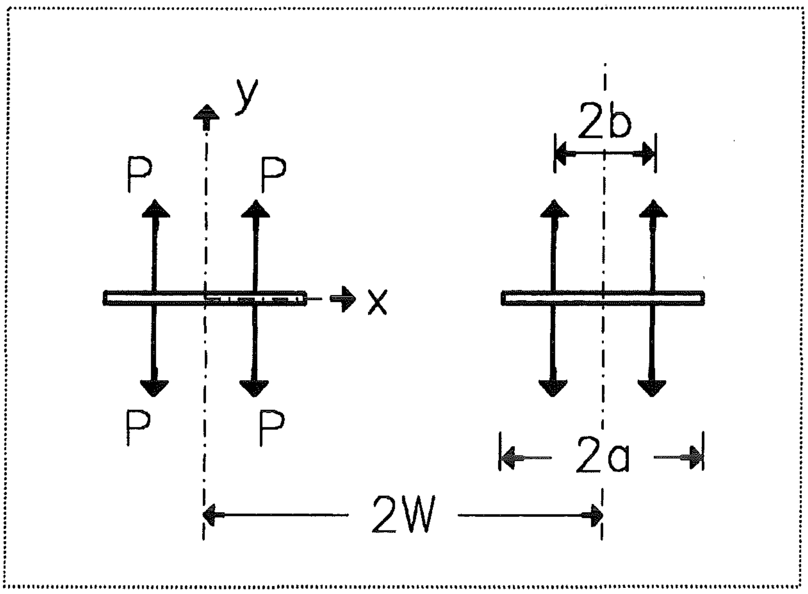

Figure 9. . Array of collinear internal cracks loaded with point forces.

$$h_{y,DE}(a,b) = h_{y,INT} + \frac{1}{P}\int_0^\infty \sigma_x(0,y,b)\, h_{x,DE}(a,y)\, dy \qquad (37)$$

We are now interested in the first derivative of the weight function directly at the free surface. Since the weight function for the internal crack is symmetric at the crack centre, $\partial h_{y,INT}/\partial b(a,b=0)=0$, we find

$$\frac{\partial h_{y,DE}(a,b)}{\partial b}\Big|_{b=0} = \frac{1}{P}\int_0^\infty h_{x,DE}(a,y)\frac{\partial \sigma_{appl}}{\partial b}\Big|_{b=0} dy \qquad (38)$$

From eq.(30) we can see that the Westergaard stress function is symmetric with respect to the real variable b. This is the case because b only occurs in the terms

$$\cos(\pi b/W)\,, \quad \sin^2(\pi b/W)$$

which are symmetric with respect to $b=0$. Consequently, it holds $\partial\Phi/\partial b=0$ and we obtain for the derivatives

$$\frac{\partial \sigma_x}{\partial b}\Big|_{b=0} = \mathrm{Re}\,\frac{\partial \Phi}{\partial b}\Big|_{b=0} - y\,\mathrm{Im}\,\frac{d}{dz}\frac{\partial \Phi}{\partial b}\Big|_{b=0} = 0 \qquad (39)$$

From eq.(38) it results

$$\frac{\partial h_{y,DE}}{\partial b}\Big|_{b=0} = 0 \tag{40}$$

3.4.2 The double-edge-cracked plate of finite height

Now we consider plates of finite height. The first derivative of the weight function is given by

$$\frac{\partial h}{\partial x}\Big|_{x=0} = \frac{E'}{K}\frac{\partial}{\partial a}\frac{\partial v}{\partial x}\Big|_{x=0} = \frac{1}{Y\sqrt{a}}\frac{\partial}{\partial a}\left(\frac{E'}{\sigma_0}\frac{\partial v}{\partial x}\Big|_{x=0}\right) \tag{41}$$

The slope of the crack opening displacement at $x = 0$ - a measure of the first derivative of the weight function (see eq.(41)) - is plotted in fig.10 for several values of L/W and a/W. In case of $L/W = 1.5$ the data are nearly independent of the relative crack length. In this case we may conclude:

$$\frac{E'}{\sigma_0}\frac{\partial v}{\partial x}\Big|_{x=0} \simeq const. \Rightarrow \frac{\partial h}{\partial x}\Big|_{x=0} \simeq 0 \tag{42}$$

If the data points of fig.10 are fitted by straight lines, we find a common limit value of about 1.58 for $a/W \to 0$. This extrapolated data point may be determined also directly. For relative crack depths $a/W \to 0$ the limit behaviour of a double-edge-cracked plate is identical with that of an edge-cracked half-space. In this case, the weight function can be obtained from a highly accurate asymptotic expansion for the crack opening displacement field under remote tension loading σ_0. Wigglesworth [13] determined the v-displacements as

$$v = \sqrt{8/\pi}\; a\, Y_0 \frac{\sigma_0}{E'} \sum_{\nu=0}^{12} C_\nu \left(1-\rho\right)^{n+1/2} \quad , \quad \rho = x/a \tag{43}$$

with the coefficients

$$\begin{array}{lll} C_0 = 1.000000 & C_1 = -0.143719 & C_2 = 0.019965 \\ C_3 = 0.019665 & C_4 = 0.011856 & C_5 = 0.006254 \\ C_6 = 0.002993 & C_7 = 0.001256 & C_8 = 0.000390 \\ C_9 = -0.00001 & C_{10} = -0.000172 & C_{11} = -0.000213 \\ & C_{12} = -0.000212 & \end{array} \tag{44}$$

Based on these displacements, one can compute a highly accurate weight function according to eq.(24)

$$h(x,a) = \sqrt{\frac{2}{\pi a}} \sum_{\nu=0}^{13} D_\nu (1-\rho)^{\nu-1/2} \tag{45}$$

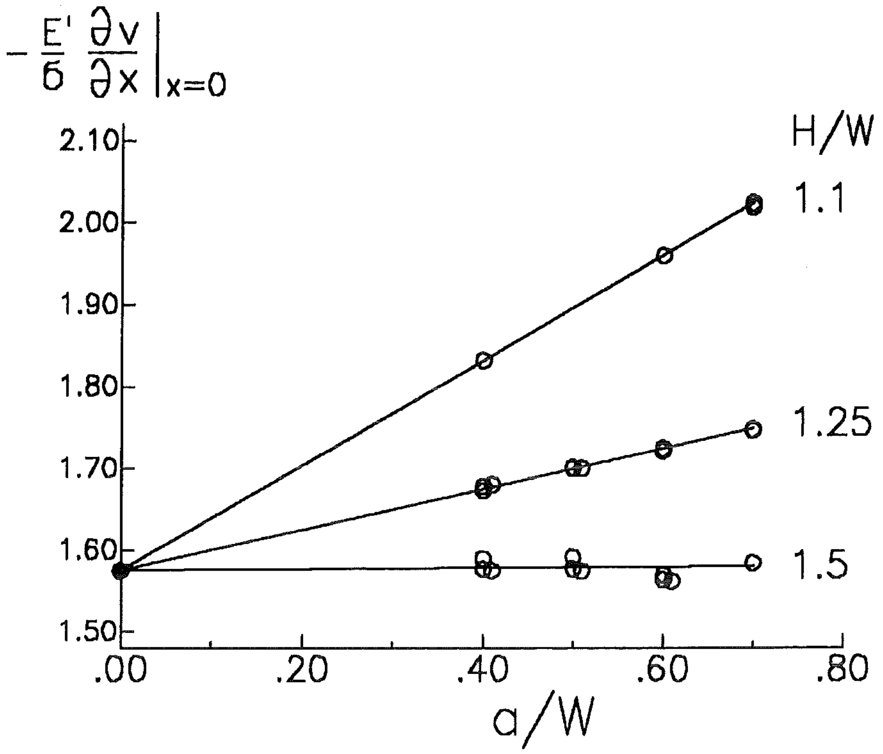

Figure 10. Derivative of displacements. First derivative of the crack opening displacement at the crack mouth.

with the coefficients

$$D_0 = 1$$

$$D_\nu = -(2\nu-3)C_{\nu-1} + (2\nu+1)C_\nu , \qquad \text{for } \ 0 < \nu \leq 12 \qquad (46)$$

$$D_{13} = -23C_{12}$$

Wigglesworth's analysis was repeated in [14] and extended up to $N = 20$ with the following coefficients

$$C_0 = 1.00000 \qquad C_1 = -0.1437181 \qquad C_2 = 0.0199656$$

$$C_3 = 0.0196651 \qquad C_4 = 0.0118558 \qquad C_5 = 0.0062537$$

$$C_6 = 0.0029935 \qquad C_7 = 0.0012562 \qquad C_8 = 0.0003899$$

$$C_9 = -0.0000097 \qquad C_{10} = -0.0001718 \qquad C_{11} = -0.0002189 \qquad (47)$$

$$C_{12} = -0.0002149 \qquad C_{13} = -0.0001909 \qquad C_{14} = -0.0001618$$

$$C_{15} = -0.0001338 \qquad C_{16} = -0.0001095 \qquad C_{17} = -0.0000893$$

$$C_{18} = -0.0000728 \qquad C_{19} = -0.0000595 \qquad C_{20} = -0.0000487$$

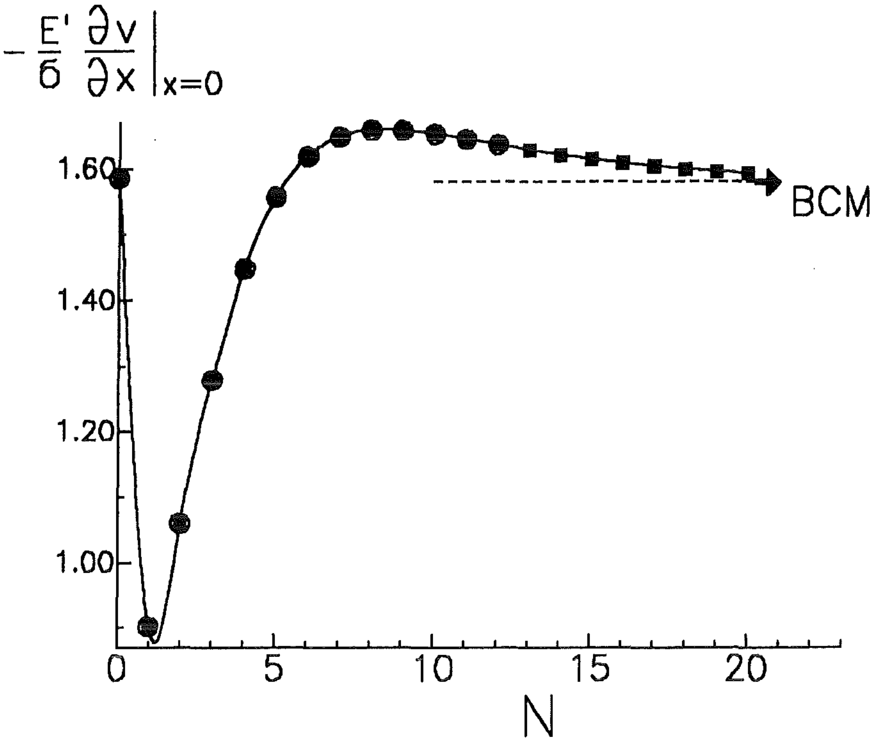

Figure 11. Derivative of displacements. First derivative of the crack opening displacement at the crack mouth for the edge-cracked half-space.

The derivative of the displacements with respect to x were computed and entered in fig.11 for an increased number of terms used in eq.(43). From the asymptotic behaviour we find the limit value of $\simeq$1.57 in agreement with the BCM-results.
From the numerical data we conclude that the disappearing first derivative of the weight function is sufficiently correct for $L/W > 1.5$.

4. References

[1] H. Bueckner, A novel principle for the computation of stress intensity factors, ZAMM **50**(1970) 529-546.

[2] T.L. Sham, Int. J. Solids and Struct. **25**(1989),357-380.

[3] T.L. Sham, Int. J. Fract. **48**(1991),81-102.

[4] T. Fett, A Green's function for T-stresses in an edge-cracked rectangular plate, submitted to Engng. Fract. Mech.

[5] T. Fett, T-stress in edge-cracked specimens, FZKA Report 5802, Forschungszentrum Karlsruhe, 1996.

[6] M.L. Williams, On the stress distribution at the base of a stationary crack, J. Appl. Mech. **24**(1957) 109-114.

[7] S.G. Larsson, A.J. Carlsson, J. of Mech. and Phys. of Solids **21**(1973),263-277.

[8] P.S. Leevers, J.C. Radon, Inherent stress biaxiality in various fracture specimen geometries, Int. J. Fract. **19**(1982),311-325.

[9] J. R. Rice, Int. J. Solids Structures **8**(1972)751-758

[10] G. Shen, G. Glinka, Determination of weight functions from reference stress intensity factors, Theor. and Appl. Fract. Mech. **15**(1991) 237-245.

[11] H.J. Petroski, J.D. Achenbach, Computation of the weight function from a stress intensity factor, Engng. Fract. Mech. **10**(1978) 257-266.

[12] H. Tada, P.C. Paris, G.R. Irwin, The stress analysis of cracks handbook, Del Research Corporation, 1986.

[13] L.A. Wigglesworth, Stress distribution in a notched plate, Mathematica **4**(1957) 76-96.

[14] T. Fett, D. Munz, Advances in stress intensity factors and weight functions, Computational Mechanics International, Southampton, 1996.